Fermilab Library
0 1160 0026881 7

November 1993 UCSD/PTH 93-40

Higher Derivative Field Theories: Applications to Particles and the Universe *

Julius Kuti[a]

Department of Physics 0319
University of California at San Diego
9500 Gilman Drive
La Jolla, CA 92093-0319 USA

Abstract

The history of higher derivative Lagrangian field theories is briefly reviewed and some applications are presented. The incompleteness problem of the scalar Higgs sector in the minimal Standard Model is replaced by a higher derivative Lagrangian, and the renormalization properties of higher derivative quantum gravity are analyzed. It is shown that logically consistent and *finite* field theories are obtained when higher derivative terms are introduced in the kinetic energy of the Lagrangian and some excitations of the fields are quantized with indefinite metric in the Hilbert space. The Landau ghost phenomenon of the triviality problem in scalar field theory is replaced by the state vectors of a complex conjugate ghost pair at some finite mass scale with observable physical consequences. A similar mechanism renders quantum gravity renormalizable and asymptotically free. It is shown that the ghost states exhibit unusual resonance properties and correspond to a complex conjugate pair of Pauli-Villars regulator masses in the euclidean path integral formulation of conventional field theories. An argument is given that microscopic acausality effects associated with the complex ghost pair remain undetectable in scattering processes with realistic wave packects, and the S-matrix exhibits unitarity in the observable sector of the Hilbert space.

*Talk presented at the 17th Johns Hopkins Workshop on *Particles and the Universe*, July 30 - August 1, 1993, Budapest, Hungary.

[a]E-mail: kuti@axpjk.ucsd.edu

FERMILAB
JAN 25 1993
LIBRARY

1 Introduction and History

In the early days of general relativity Weyl and Eddington suggested to replace the Einstein equations for the gravitational field by higher than second order field equations [1]. Although speculations along this line were not developed into a successful physical theory, interest in higher derivative Lagrangian field theories continued to grow. Some highlights of the progress will be discussed in this introductory section.

1.1 Bopp-Podolsky Electrodynamics

In a serious effort to eliminate divergent quantities in the theory of electromagnetism Bopp [2] and Podolsky [3] proposed a higher derivative extension of the Maxwell equations. Their idea can be illustrated in the following simple way. Consider the non-relativistic modification of the electrostatic Lagrangian,

$$L = \frac{1}{8\pi} \int \left[\vec{E}^2 + a^2 (\nabla \vec{E})^2 \right] d^3 r \quad , \tag{1}$$

which leads to the higher deirvative electrostatic equation

$$\left(1 - a^2 \triangle\right) \triangle \Phi = -4\pi\rho \quad . \tag{2}$$

The solution of Eq. 2 in the presence of a pointlike static charge q with $\rho = q\delta(\vec{r})$ can be written as

$$\phi = \frac{q}{r}(1 - e^{-r/a}) \quad . \tag{3}$$

In Eq. 3 the coefficient a of the higher derivative term acts as a static screening length, or cutoff. The modification of the Maxwell Lagrangian eliminated the singularity of the electrostatic Coulomb potential at the origin. It was hoped, therefore, that the higher derivative Lagrangian will cure the classical and quantum divergences of electrodynamics. This program, however, required a relativistic generalization and a consistent quantization procedure.

The relativistic generalization of Eq. 1 is straightforward. The Lagrangian is given by

$$L = -\frac{1}{4} F_{\mu\nu} F^{\mu\nu} - \frac{1}{4} \Lambda^{-2} \Box F_{\mu\nu} \Box F^{\mu\nu} \quad , \tag{4}$$

where $F_{\mu\nu}$ designates the electromagnetic field strength tensor, and the notation $a^{-1} = \Lambda$ is used. In addition to massless photon excitations, the higher derivative modification of the Maxwell Lagrangian in Eq. 4 describes a heavy photon whose mass m is related to the inverse screening length (cutoff) by the simple relation $m = \hbar\Lambda/c$.

1.2 Hilbert Space with Indefinite Metric

Higher derivative quantum field theories were studied by Pais and Uhlenbeck [4] in a general context. Their observations are also directly applicable to the Lagrangian of Eq. 4. Higher derivative theories have new degrees of freedom with negative energy excitations. The heavy photon of the higher derivative Maxwell Lagrangian is an illustration. It represents the new and negative energy excitation in the theory. The conventional quantization procedure fails in this case. The negative energy excitations can grow indefinitely with increasing frequencies and there is no stable ground state in the quantized field system. The classical analogue of this instability is the presence of some runaway solutions of the higher derivative field equations. Indefinite metric quantization of the negative energy modes is a remedy for the instability problem. All excitations will have positive energies but some of the new degrees of freedom correspond to negative metric states in the Hilbert space. This is the famous ghost problem which can destroy the unitarity of the S-matrix.

Lee and Wick investigated the problem of negative norm states and the unitarity of the S-matrix in their full complexity [5]. They studied Quantum Electrodynamics in the presence of the heavy photon which is represented by a state vector of negative norm in the Hilbert space. They pointed out that the heavy photon, which has real energy without coupling to charged matter, splits into a complex conjugate pole pair on the first Riemann sheet of the elastic electron-positron scattering amplitude. Lee and Wick conjectured that this complex ghost pair does not violate the unitarity properties of the S-matrix in physical processes.

Based on the investigation of a higher derivative scalar field theory with self-interaction I will argue that the Lee-Wick conjecture can be derived from first principles. It will be shown that logically consistent and *finite* field theories are obtained when higher derivative terms are introduced in the kinetic energy of the Lagrangian and some excitations of the fields are quantized with indefinite metric in the Hilbert space. The Landau ghost phenomenon of the triviality problem in scalar field theory is replaced by the state vectors of a complex conjugate ghost pair at some finite mass scale with observable physical consequences. A similar mechanism renders quantum gravity renormalizable and asymptotically free. It will be shown that the ghost states exhibit unusual resonance properties and correspond to a complex conjugate pair of Pauli-Villars regulator masses in the euclidean path integral formulation of conventional field theories. An argument is given that microscopic acausality effects associated with the complex ghost pair remain undetectable in scattering processes with realistic wave packects, and the S-matrix exhibits unitarity in the observable

sector of the Hilbert space.

1.3 Higher Derivative Quantum Gravity

The higher derivative theory of quantum gravity is a renormalizable field theory with very interesting mathematical and physical properties [6, 7]. The Lagrangian which is quadratic in the curvature has three independent terms,

$$S = -\int d^4x\sqrt{-g}\Big\{\frac{\gamma}{\kappa^2}R + \alpha R_{\mu\nu}R^{\mu\nu} - \beta R^2\Big\} \quad . \tag{5}$$

The first term in Eq. 5 with $\gamma = 2$ corresponds to the original Einstein-Hilbert action with second order derivatives in the metric tensor $g_{\mu\nu}$. The last two terms, expressed in terms of fourth order derivatives of the metric tensor, are in the class of higher derivative field theories. Although the higher derivative terms in the action have very little effect on the low-frequency domain of classical experiments, at high frequencies they dominate the quantum behavior of the theory. They provide the stabilization of the divergence structure at short distances, with power-counting renormalizability of the quantum loops.

Some of the important features of higher derivative quantum gravity will be discussed later. The excitation spectrum has to be investigated together with the quantization rules in a Hilbert space with negative norm states. The short distance behavior of quantum fluctuations exhibits asymptotic freedom in the couplings. It remains a challenge to understand the crossover from the new short distance physics to the long range behavior of Einstein's general relativity.

One might speculate that the higher derivative action of Eq. 5 is simply some low-energy approximation to a new and more sophisticated theory of quantum gravity on the Planck scale. The connection between higher derivative Lagrangian theories and effective low-energy expansions is a somewhat ambiguous notion. The last part of this introduction illustrates the problem in a simple toy model.

1.4 Effective Field Theories

Consider two coupled harmonic oscillators with the Lagrangian

$$L = \frac{1}{2}\dot{x}^2 - \frac{1}{2}\omega^2 x^2 + \frac{1}{2}\dot{\xi}^2 - \frac{1}{2}\Omega^2\xi^2 - g\omega^2 x\xi \quad , \tag{6}$$

where x is the dynamical variable of the low-frequency (ω) oscillator, and ξ designates the coordinate variable of the high-frequency (Ω) oscillator. The coupling strength g between the two oscillators is arbitrary. Integration over

the high-frequency modes leads to an effective theory in the variable x,

$$\int \mathcal{D}(\xi) \int \mathcal{D}(x) e^{\frac{i}{\hbar}\int L(x,\dot{x},\xi,\dot{\xi})dt} = \int \mathcal{D}(x) e^{\frac{i}{\hbar}\int L_{eff}(x,\dot{x})dt} \quad , \tag{7}$$

where

$$L_{eff} = \frac{1}{2}\dot{x}^2 - \frac{1}{2}\omega^2 x^2 + \frac{1}{2}g^2\omega^2 x \frac{\omega^2}{\frac{d^2}{dt^2} + \Omega^2} x \quad . \tag{8}$$

The last term is recognized as the non-local effect of the high-frequency oscillator on the dynamics of x. The non-local effective Lagrangian in Eq. 8 is exact. At very low frequencies L_{eff} can be approximated by a power series expansion of the non-local operator,

$$L_{eff} = \frac{1}{2}\dot{x}^2 - \frac{1}{2}\omega^2 x^2 + \frac{1}{2}g^2\frac{\omega^4}{\Omega^2}x^2 - \frac{1}{2}g^2\frac{\omega^4}{\Omega^4}x\frac{d^2x}{dt^2} + \frac{1}{2}g^2\frac{\omega^4}{\Omega^6}x\frac{d^4x}{dt^4} + ... \tag{9}$$

where the higher derivative terms are organized according to increasing powers of $1/\Omega^2$. The higher dimensional operators, which appear as corrections to the original oscillator Lagrangian of x, have small effects at low frequencies and they can be treated perturbatively. One can also construct a higher derivative Lagrangian where the infinite number of terms designated by the ellipsis are truncated. This Lagrangian can be subjected to a full quantization procedure as it will be described in the next section. This higher derivative theory approximates the original theory at low energies. However, the truncated effective expansion breaks down at the energy scale $E \approx \hbar\Omega$ and the higher derivative Lagrangian will not approximate the exact L_{eff} of Eq. 8 at large frequencies. The quantization procedure when applied to the truncated Lagrangian as a higher derivative theory will introduce new physics on the energy scale $\hbar\Omega$, like ghost states, which were not part of the exact non-local effective Lagrangian in Eq. 8.

2 The Quantization Procedure

The canonical quantization procedure for higher derivative field theories will be described in this section starting from the method of Ostrogradski [8]. Indefinite metric will be introduced in the Hilbert space of the state vectors to secure a stable ground state and positive energy excitations. The mathematical properties and physical consequences of complex conjugate ghost pairs with state vectors of negative norm will be discussed. A simple quantum mechanical model illustrates the strategy of our approach [10, 11].

2.1 Quantum Mechanics

Consider the classical Lagrangian of a non-relativistic particle moving in one dimension:

$$L = \frac{1}{2}\Big(1+\frac{2\omega^2}{M^2}\cos 2\Theta\Big)\dot{x}^2 - \frac{1}{M^2}\Big(\cos 2\Theta + \frac{\omega^2}{2M^2}\Big)\ddot{x}^2 + \frac{1}{2M^4}\dddot{x}^2 - \frac{1}{2}\omega^2 x^2 \ . \quad (10)$$

Eq. 10 describes a simple harmonic oscillator with second and third derivative terms added to the original Lagrangian whose potential energy term is $V(x) = 1/2\ \omega^2 x^2$; M and ω are measured in units of the Newton mass m of the original oscillator particle, set to $m = 1$ for convenience. For simple interpretation of the results, the coefficients of the derivative terms are given in terms of M and an angle parameter Θ; the only restrictions imposed are $\omega^2/M^2 < 1$ and $0 < \Theta < \pi/2$.

If an additional term, proportional to $x d^6x/dt^6$, had been displayed in Eq. 9 before truncation, the derivative structure of the Lagrangian in Eq. 10 would match the displayed terms by partial integration. The parametrization of the Lagrangian L in Eq. 10 differs from the parametrization of L_{eff} , since we are considering an independent and self-contained higher derivative Lagrangian model.

The variational principle leads to the higher order Euler-Lagrange equation of motion,

$$\frac{1}{M^4}\frac{d^6x}{dt^6} + \frac{2}{M^2}\Big(\cos 2\Theta + \frac{\omega^2}{2M^2}\Big)\frac{d^4x}{dt^4} - \Big(1+\frac{2\omega^2}{M^2}\cos 2\Theta\Big)\frac{d^2x}{dt^2} + \omega^2 x = 0 \ , \quad (11)$$

which differs from Newton's equation by higher derivative terms with small coefficients in the limit $\omega^2/M^2 \ll 1$, and $1/M^2 \ll 1$ (limit of large regulator masses in field theory). Even very small higher derivative terms will have, however, a qualitative impact on the theory, as shown in the following analysis.

The canonical formalism for higher derivative theories was developed first by Ostrogradski [8, 4]. Three independent generalized coordinates x, $\dot{x}$, and $\ddot{x}$ are introduced and the generalized canonical momenta are defined by

$$\pi_x = \frac{\partial L}{\partial \dot{x}} - \frac{d}{dt}\frac{\partial L}{\partial \ddot{x}} + \frac{d^2}{dt^2}\frac{\partial L}{\partial \dddot{x}} =$$
$$\Big(1+\frac{2\omega^2}{M^2}\cos 2\Theta\Big)\dot{x} + \frac{2}{M^2}\Big(\cos 2\Theta + \frac{\omega^2}{2M^2}\Big)\dddot{x} + \frac{1}{M^4}\frac{d^5x}{dt^5} \ ,$$

$$\pi_{\dot{x}} = \frac{\partial L}{\partial \ddot{x}} - \frac{d}{dt}\frac{\partial L}{\partial \dddot{x}} = -\Big(\frac{2\cos 2\Theta}{M^2} + \frac{\omega^2}{M^4}\Big)\ddot{x} - \frac{1}{M^4}\frac{d^4x}{dt^4},$$

$$\pi_{\ddot{x}} = \frac{\partial L}{\partial \dddot{x}} = \frac{1}{M^4}\dddot{x} \ . \quad (12)$$

With Ostrogradski's method we find the Hamiltonian

$$H = \pi_x \cdot \dot{x} + \pi_{\dot{x}} \cdot \ddot{x} + \frac{1}{2}M^4\pi_{\ddot{x}}^2 + \frac{1}{2}\omega^2 x^2$$
$$- \frac{1}{2}\Big(1 + 2\frac{\omega^2}{M^2}\cos 2\Theta\Big)\dot{x}^2 + \frac{1}{2}\Big(\frac{\omega^2}{M^4} + \frac{2\cos 2\Theta}{M^2}\Big)\ddot{x}^2. \tag{13}$$

In quantum mechanics the operators of the canonical variables satisfy standard Heisenberg commutation relations,

$$[\hat{x}, \hat{\pi}_x] = i\hbar \ , \qquad [\hat{\dot{x}}, \hat{\pi}_{\dot{x}}] = i\hbar \ , \qquad [\hat{\ddot{x}}, \hat{\pi}_{\ddot{x}}] = i\hbar \ . \tag{14}$$

All the other commutators of the six operators vanish. We define the Hilbert space with indefinite metric by the scalar product [9]

$$\langle x', \dot{x}', \ddot{x}' | x, \dot{x}, \ddot{x}\rangle = \delta(x' - x)\ \delta(\dot{x}' + \dot{x})\ \delta(\ddot{x}' - \ddot{x}) \ , \tag{15}$$

as indicated by the *plus sign* in the second δ-function on the right side of Eq. 15. The wave function $\psi(x, \dot{x}, \ddot{x}) = \langle x, -\dot{x}, \ddot{x}|\psi\rangle$ depends on the three independent generalized coordinates. The completeness relation in the indefinite metric Hilbert space is given by

$$\int dx \int d\dot{x} \int d\ddot{x}\ |x, -\dot{x}, \ddot{x}\rangle\langle x, \dot{x}, \ddot{x}| = \mathrm{I} \ . \tag{16}$$

The representation of the self-adjoint operators $\hat{x}, \hat{\pi}_x$, $\hat{\dot{x}}, \hat{\pi}_{\ddot{x}}$ follows the rules of ordinary quantum mechanics, $\hat{x}\ \psi = x \cdot \psi$, $\hat{\pi}_x\ \psi = -i\hbar\ \frac{\partial\psi}{\partial x}$, and similarly, $\hat{\dot{x}}\ \psi = \ddot{x} \cdot \psi$, $\hat{\pi}_{\ddot{x}}\ \psi = -i\hbar\ \frac{\partial\psi}{\partial\ddot{x}}$. However, $\hat{\dot{x}}$ and $\hat{\pi}_{\dot{x}}$ (also self-adjoint with respect to the indefinite metric) are represented by $\hat{\dot{x}}\ \psi = i\dot{x} \cdot \psi$, and $\hat{\pi}_{\dot{x}}\ \psi = -\hbar\frac{\partial\psi}{\partial\dot{x}}$ [9].

The euclidean partition function in the presence of external sources is defined by

$$\begin{aligned} Z_T(J_0, J_1, J_2) &= \mathrm{Tr} e^{-\frac{1}{\hbar}TH} \\ &= \int dx \int d\dot{x} \int d\ddot{x}\ \langle x, -\dot{x}, \ddot{x}| e^{-\frac{1}{\hbar}TH} |x, \dot{x}, \ddot{x}\rangle \ , \end{aligned} \tag{17}$$

where a time-dependent source term $J_0\hat{x} + J_1\hat{\dot{x}} + J_2\hat{\ddot{x}}$ is included in the Hamiltonian. The partition function of Eq. 17 can be written as a Hamiltonian path integral in six canonical variables. After integrating over $\dot{x}, \ddot{x}, \pi_x, \pi_{\dot{x}}, \pi_{\ddot{x}}$, we find [10, 11]

$$Z_T(J_0, J_1, J_2) = \int d[x(\tau)]\ \exp\Big\{-\frac{1}{\hbar}\int_0^T d\tau \Big(L_E + J_0(\tau)x(\tau)$$
$$+ J_1(\tau)\frac{dx}{d\tau} + J_2(\tau)\frac{d^2x}{d\tau^2}\Big)\Big\}, \tag{18}$$

where L_E is the *euclidean* Lagrangian of the higher derivative model,

$$L_E = \left(\frac{1}{2} + \frac{\omega^2}{M^2}\cos 2\Theta\right)\left(\frac{dx}{d\tau}\right)^2 + \frac{1}{2}\omega^2 x^2(\tau) + \frac{1}{M^2}\left(\cos 2\Theta + \frac{\omega^2}{2M^2}\right)\left(\frac{d^2x}{d\tau^2}\right)^2 + \frac{1}{2}M^{-4}\left(\frac{d^3x}{d\tau^3}\right)^2 . \tag{19}$$

In the T $\longrightarrow \infty$ limit, after the evaluation of the path integral in Eq. 18, we obtain

$$Z_\infty(\tilde{J}_0(E), \tilde{J}_1(E), \tilde{J}_2(E)) = Z_\infty(0,0,0) \times \exp\left\{-\frac{1}{2}\int dE \tilde{J}(E)\widetilde{D}(E)\tilde{J}(-E)\right\} , \tag{20}$$

where $\tilde{J}(E) = \tilde{J}_0(E) - iE\tilde{J}_1(E) - E^2\tilde{J}_2(E)$. The Fourier transform of the quantum mechanical propagator $D(\tau)$ is given by

$$\widetilde{D}(E) = \frac{M^4}{(E^2+\omega^2)(E^2+M^2e^{2i\Theta})(E^2+M^2e^{-2i\Theta})} . \tag{21}$$

The physical significance of the multiple pole structure in the propagator becomes clear from the spectrum of the Hamiltonian which can be transformed to a diagonal form,

$$H = \hbar\left[\omega a^{(+)}a^{(-)} + Me^{i\Theta}b^{(+)}b^{(-)} + Me^{-i\Theta}c^{(+)}c^{(-)} + \frac{1}{2}(\omega + Me^{i\Theta} + Me^{-i\Theta})\right] . \tag{22}$$

The creation operators $a^{(+)}, b^{(+)}, c^{(+)}$ and the annihilation operators $a^{(-)}, b^{(-)}$, $c^{(-)}$ are linear combinations of the six canonical variables $x, \dot{x}, \ddot{x}, \pi_x, \pi_{\dot{x}}, \pi_{\ddot{x}}$ with commutation relations $[a^{(-)}, a^{(+)}] = 1$, $[b^{(-)}, b^{(+)}] = 1$, $[c^{(-)}, c^{(+)}] = 1$. All the other commutators vanish. The adjoint of $a^{(+)}$ is $\overline{a^{(+)}} = a^{(-)}$, and similarly, $\overline{b^{(+)}} = c^{(-)}$, $\overline{c^{(+)}} = b^{(-)}$.

The eigenstates of the Hamiltonian are given by

$$|l,m,n\rangle = \frac{1}{\sqrt{n!}}(c^{(+)})^n\frac{1}{\sqrt{m!}}(b^{(+)})^m\frac{1}{\sqrt{l!}}(a^{(+)})^l\,|0,0,0\rangle , \tag{23}$$

where the ground state $|0,0,0\rangle$ is annihilated by $a^{(-)}$, $b^{(-)}$, $c^{(-)}$. The complex energy eigenvalues

$$E_{l,m,n} = (l+\frac{1}{2})\hbar\omega + (m+\frac{1}{2})\hbar Me^{i\Theta} + (n+\frac{1}{2})\hbar Me^{-i\Theta} \tag{24}$$

satisfy the symmetry relation $E_{l,m,n} = E^*_{l,n,m}$. In addition to the ordinary oscillator excitations we have two conjugate ghost oscillators with complex energies, in agreement with the two new degrees of freedom in the Lagrangian.

The energy eigenstates have indefinite metric normalization,

$$\langle l', m', n' | l, m, n \rangle = \delta_{l'l} \delta_{m'n} \delta_{n'm} \ . \tag{25}$$

For $m = n$, the ghost oscillator and its complex conjugate partner are excited in pairs and the corresponding state vectors have positive norm with real energy. However, unbalanced ghost excitations with $m \neq n$ correspond to zero norm state vectors with complex energies. Some linear combinations of ghost excitations with $m \neq n$ will have negative norm.

The quantization procedure we developed has several important consequences. The euclidean propagator $\widetilde{D}(E)$ of Eq. 21 can be written as a sum of three simple pole terms describing the original oscillator and the complex conjugate pair of ghost oscillators. The conjugate ghost poles play the same role as the auxiliary Pauli-Villars regulators in field theory. The method, which is applicable for any potential energy $V(x)$ in the Lagrangian of Eq. 10, leads to the euclidean path integral formulation of Eq. 18 providing a non-perturbative framework for numerical investigations [10, 11]. The euclidean path integral, however, cannot be continued to real time since the Wick rotation of the integration contour is blocked by the complex ghost poles on the first sheet of the complex energy plane. The ghost eigenstates with complex energies represent run-away time evolution in the Hilbert space rendering the real-time path integral ill-defined. At the same time, the hamiltonian approach remains well-defined in the indefinite metric Hilbert space and provides the theoretical foundation of the model in real time. Important informations can also be extracted directly from the euclidean path integral of Eq. 18.

2.2 Scalar Field Theory

As the first example of the canonical quantization procedure in higher derivative field theory consider the scalar field $\phi_\alpha(\vec{x}, t)$ with an internal index $\alpha = 1, 2, ..., 4$ for the purpose of later applications. The Lagrangian is defined as

$$L = \frac{1}{2} \partial_\mu \vec{\phi} \partial^\mu \vec{\phi} + \frac{1}{2M^4} \Box \partial_\mu \vec{\phi} \, \Box \partial^\mu \vec{\phi} - \frac{1}{2} m_0^2 \vec{\phi} \cdot \vec{\phi} - \lambda_0 \left(\vec{\phi} \cdot \vec{\phi} \right)^2 \ . \tag{26}$$

The notation $\vec{\phi}$ indicates that the scalar field transforms as a vector under the O(4) symmetry of the Lagrangian. Following the procedure of Ostrogradski three independent field variables (generalized coordinates) $\phi_\alpha(\vec{x}, t)$, $\dot{\phi}_\alpha(\vec{x}, t)$, and $\ddot{\phi}_\alpha(\vec{x}, t)$, $\alpha = 1, 2, 3, 4$ are chosen at each point $\vec{x}$ in the three-dimensional coordinate space . The notation $\dot{\phi}_\alpha(\vec{x}, t)$ stands for the first partial time derivative of $\phi_\alpha(\vec{x}, t)$; $\ddot{\phi}_\alpha(\vec{x}, t)$ designates the second partial time derivative.

The canonical field momentum variables Π_{ϕ_α}, $\Pi_{\dot{\phi}_\alpha}$, $\Pi_{\ddot{\phi}_\alpha}$ are defined in close analogy with Eq. 12. The Heisenberg commutators of the canonical field and momentum variables have the same form as in ordinary quantum field theory with positive definite metric, similarly to the quantum mechanical case of Eq. 14. The state vectors $|\psi\rangle$ are described by wave functionals in the field-diagonal representation of the indefinite metric Hilbert space,

$$\psi\Big\{\phi_\alpha(\vec{x}), \dot{\phi}_\alpha(\vec{x}), \ddot{\phi}_\alpha(\vec{x})\Big\} = \langle \phi_\alpha(\vec{x}), -\dot{\phi}_\alpha(\vec{x}), \ddot{\phi}_\alpha(\vec{x})|\psi\rangle \ . \tag{27}$$

The operators $\hat{\phi}_\alpha$, $\hat{\Pi}_{\phi_\alpha}$ are represented in the Hilbert space conventionally,

$$\hat{\phi}_\alpha(\vec{x})\ \psi\Big\{\phi_\alpha(\vec{x}), \dot{\phi}_\alpha(\vec{x}), \ddot{\phi}_\alpha(\vec{x})\Big\} = \phi_\alpha(\vec{x}) \cdot \psi\Big\{\phi_\alpha(\vec{x}), \dot{\phi}_\alpha(\vec{x}), \ddot{\phi}_\alpha(\vec{x})\Big\}, \tag{28}$$

$$\hat{\Pi}_{\phi_\alpha}\ \psi\Big\{\phi_\alpha(\vec{x}), \dot{\phi}_\alpha(\vec{x}), \ddot{\phi}_\alpha(\vec{x})\Big\} = -i\hbar\frac{\delta}{\delta\phi_\alpha(\vec{x})}\ \psi\Big\{\phi_\alpha(\vec{x}), \dot{\phi}_\alpha(\vec{x}), \ddot{\phi}_\alpha(\vec{x})\Big\}, \tag{29}$$

with similar representation for the $\hat{\ddot{\phi}}_\alpha$, $\hat{\Pi}_{\ddot{\phi}_\alpha}$ operator pair. However, the representation of the $\hat{\dot{\phi}}_\alpha$, $\hat{\Pi}_{\dot{\phi}_\alpha}$ pair reveals the indefinite metric [10, 11],

$$\hat{\dot{\phi}}_\alpha(\vec{x})\ \psi\Big\{\phi_\alpha(\vec{x}), \dot{\phi}_\alpha(\vec{x}), \ddot{\phi}_\alpha(\vec{x})\Big\} = i\ \dot{\phi}_\alpha(\vec{x}) \cdot \psi\Big\{\phi_\alpha(\vec{x}), \dot{\phi}_\alpha(\vec{x}), \ddot{\phi}_\alpha(\vec{x})\Big\}\ , \tag{30}$$

$$\hat{\Pi}_{\dot{\phi}_\alpha}\ \psi\Big\{\phi_\alpha(\vec{x}), \dot{\phi}_\alpha(\vec{x}), \ddot{\phi}_\alpha(\vec{x})\Big\} = -\hbar\frac{\delta}{\delta\dot{\phi}_\alpha(\vec{x})}\ \psi\Big\{\phi_\alpha(\vec{x}), \dot{\phi}_\alpha(\vec{x}), \ddot{\phi}_\alpha(\vec{x})\Big\}\ . \tag{31}$$

Following the canonical procedure of the quantum mechanical model, the Hamilton operator can be expressed in terms of the field variables $\phi_\alpha(\vec{x})$, $\dot{\phi}_\alpha(\vec{x})$, $\ddot{\phi}_\alpha(\vec{x})$ and the canonical field momentum variables $\Pi_{\phi_\alpha}(\vec{x})$, $\Pi_{\dot{\phi}_\alpha}(\vec{x})$, $\Pi_{\ddot{\phi}_\alpha}(\vec{x})$. The euclidean partition function $Z_T = \mathrm{Tr}e^{-\frac{1}{\hbar}TH}$ is represented by a Hamiltonian path integral in the six canonical variables. It is straightforward to derive the conventional euclidean path integral by integrating over the variables $\dot{\phi}_\alpha$, $\ddot{\phi}_\alpha$, Π_{ϕ_α}, $\Pi_{\dot{\phi}_\alpha}$, $\Pi_{\ddot{\phi}_\alpha}$. In the $T \to \infty$ limit we find

$$Z = \int [d\vec{\phi}]\ \exp\ \Big\{-\frac{1}{\hbar}S_E[\vec{\phi}]\Big\}\ , \tag{32}$$

where the euclidean action S_E is given by

$$S_E = \int d^4x\Big[-\frac{1}{2}\ \vec{\phi}\ (\Box + \frac{1}{M^4}\Box^3)\ \vec{\phi} + \frac{1}{2}m_0^2\ \vec{\phi}\cdot\vec{\phi} + \lambda_0(\vec{\phi}\cdot\vec{\phi})^2\ \Big]\ , \tag{33}$$

and $\Box$ is the euclidean Laplace operator in four dimensions. The higher derivative term $M^{-4}\Box^3$ acts in the inverse euclidean propagator as a Pauli-Villars regulator with mass parameter M. It represents a minimal modification of the

continuum model, if we want to render the field theory and its euclidean path integral finite. Like in higher derivative quantum mechanics, the euclidean propagator is the sum of three simple poles: a complex conjugate pair of ghost poles is added to the simple pole representing the original O(4) particle.

The general particle content of the model is exhibited by the Hamiltonian in terms of creation and annihilation operators, $H = H_0 + H_{int}$,

$$H_0 = \sum \hbar \Big[\omega(\vec{p}) a_\alpha^{(+)}(\vec{p}) a_\alpha^{(-)}(\vec{p}) + \Omega(\vec{p}) b_\alpha^{(+)}(\vec{p}) b_\alpha^{(-)}(\vec{p}) + \Omega^*(\vec{p}) c_\alpha^{(+)}(\vec{p}) c_\alpha^{(-)}(\vec{p}) \Big] , \tag{34}$$

where the summation is over internal O(4) indices and momentum modes. The dispersion of the massive O(4) particle is given by $\omega(\vec{p}) = \sqrt{\vec{p}^2 + m_0^2}$ and the complex energy of the ghost state is $\Omega(\vec{p}) = \sqrt{\vec{p}^2 + \mathcal{M}^2}$, with $\mathcal{M} = M \cdot e^{i\Theta}$. In a more conventional parametrization one separates the real and imaginary parts, $\mathcal{M} = \mu + i\gamma/2$, $\mu = M\cos\Theta$, $\gamma = 2M\sin\Theta$. The form of the Lagrangian in Eq. 26 determines the complex phase Θ as a specific function of m_0 and M. With the addition of a $\Box^2$ term to the Lagrangian the phase angle Θ can be promoted to an independent parameter moving the ghost pair on the complex energy plane without restrictions. We will assume $\tan\Theta \approx 1$, so that γ is of the same order of magnitude as μ in our applications.

The operator $a_\alpha^{(+)}(\vec{p})$ creates the original O(4) particle with momentum $\vec{p}$ and energy $\hbar\omega(\vec{p})$. The operator $b_\alpha^{(+)}(\vec{p})$ creates a ghost state with momentum $\vec{p}$ and complex energy $\hbar\Omega(\vec{p})$; $c_\alpha^{(+)}(\vec{p})$ creates the complex conjugate ghost state. The commutation relations of the creation and annihilation operators, their conjugation properties, and the metric properties of the states they create are obtained in full analogy with the higher derivative quantum mechanical oscillator. The interaction part of the Hamiltonian is proportional to the coupling constant and expressed in terms of creation and annihilation operators.

The hamiltonian formulation and the euclidean path integral framework we derived provide self-contained non-perturbative tools for further investigations [10, 11]. In earlier work Slavnov introduced a formal path integral in Minkowski space-time, based on a canonical quantization procedure [12]. The complex ghost states with run-away time evolution render the Minkowski path integral ill-defined and inadequate for non-perturbative analysis. Hawking based his work [13] on the euclidean path integral approach as an intuitive starting point without establishing the important connection with the canonical quantization procedure.

3 Ghosts and Unitarity

The anatomy of a complex ghost state and the unitarity properties of scattering amplitudes will be discussed in this section. The mathematical properties and physical consequences of complex ghost poles in scattering amplitudes will be illustrated first in the simple Wigner-Weisskopf model [14].

3.1 Wigner-Weisskopf Model

Consider a static object in three-dimensional space, located at the origin of the coordinate system. We assign mass M and two intrinsic states, labelled by 0 and 1, to the object. When this motionless heavy particle is in its intrinsic state 0, a nonrelativistic particle of mass m is also present and described by the Schrödinger equation. When the static particle is in its intrinsic state 1, the Schrödinger particle of mass m is not present. The vectors of the Hilbert space have two orthogonal subspaces. The vector $|0;\vec{r}\rangle$ describes the heavy object at the origin in state 0 and the Schrödinger particle at some position $\vec{r}$. The state vector $|1;0\rangle$ corresponds to the heavy particle in state 1 without the light particle present. The static particle can change its intrinsic state from 0 to 1 by absorbing the Schrödinger particle, and from 1 to 0 by reemitting it with a form factor $\Lambda(\vec{r})$. The Hamiltonian $H = H_0 + V$ is given by

$$\begin{aligned} H_0 &= \int d^3\vec{p}\Big(\frac{\vec{p}^{\,2}}{2m}\Big)|0;\vec{p}\rangle\langle 0;\vec{p}| + M|1;0\rangle\langle 1;0| \ , \\ V &= g\Big(|0;\chi\rangle\langle 1;0| + |1;0\rangle\langle 0;\chi|\Big) \ , \end{aligned} \tag{35}$$

where g is a coupling constant and $\Lambda(\vec{r}) = \langle 0;\vec{r}|0;\chi\rangle$ is the form factor which was mentioned before. The orthogonality properties of the state vectors are conventional,

$$\begin{aligned} \langle 1,0|1,0\rangle &= 1 \ , \\ \langle 0;\vec{p}|0;\vec{q}\rangle &= \delta^{(3)}(\vec{p}-\vec{q}) \ . \end{aligned} \tag{36}$$

The Lippmann-Schwinger equation

$$|\Psi^{(+)}_{\vec{p}}\rangle = |0;\vec{p}\rangle + \lim_{\epsilon\to 0}\frac{1}{E_{\vec{p}} - H_0 + i\epsilon}V|\Psi^{(+)}_{\vec{p}}\rangle \ , \tag{37}$$

with $E_{\vec{p}} = \vec{p}^{\,2}/2m$, describes the scattering of the Schrödinger particle on the heavy object. The solution of Eq. 37 with a spherically symmetric form factor $\Lambda(r)$ corresponds to s-wave scattering and the exact scattering amplitude is

given by

$$t(p) = \frac{-\frac{1}{2}\Gamma(p)}{E - E_R(p) + \frac{i}{2}\Gamma(p)} , \tag{38}$$

where

$$\begin{aligned} E_R(p) &= M + g^2 4\pi m \; P\int_0^\infty dx\sqrt{2mx}\frac{|\tilde{\Lambda}(x)|^2}{x_0 - x} , \\ \Gamma(p) &= 8g^2\pi^2 mp|\tilde{\Lambda(x)}|^2 , \quad x = \frac{p^2}{2m} . \end{aligned} \tag{39}$$

In Eq. 39 $\tilde{\Lambda}$ designates the Fourier transform of the form factor and $P\int$ is the principal value of the integral. It is easy to see that there is a narrow resonance in the scattering amplitude $t(p)$ at weak coupling. The resonance energy is close to M for small g, and the width Γ is proportional to g^2. The phase shift $\delta(E)$ rapidly changes from 0 to π near $E \approx M$ with a time delay $t_D = d\delta(E)/dE \approx \Gamma^{-1}$ in the emergence of the scattered wave. The resonance pole is located on the second Riemann sheet of the scattering amplitude in the complex energy plane E.

It is easy to work out the scattering process in the same model with indefinite metric Hilbert space [15]. In this case negative norm is assigned to the state vector of the static particle when the Schrödinger particle is absent, $\langle 1,0|1,0\rangle = -1$. The other state vectors $|0;\vec{p}\rangle$ have positive norm. In the new Hamiltonian $H = H_0 + V$ the free part H_0 is given by

$$H_0 = \int d^3\vec{p}\Big(\frac{\vec{p}^{\,2}}{2m}\Big)|0;\vec{p}\rangle\langle 0;\vec{p}| - M|1;0\rangle\langle 1;0| , \tag{40}$$

and V is the same as in Eq. 35. Note the sign change of the second term in Eq. 40 when compared with Eq. 35. It is easy to see that the Hamiltonian remains self-adjoint in the indefinite metric Hilbert space. The state vector $|1;0\rangle$ with negative norm is an eigenstate of H_0 with positive eigenvalue M.

One can solve again the Lippmann-Schwinger equation with the incoming state $|0;\vec{p}\rangle$ [15]. For a spherically symmetric form factor $\Lambda(r)$ the exact scattering amplitude in the s-wave has the form

$$t(p) = \frac{\frac{1}{2}\Gamma(p)}{E - E_R(p) - \frac{i}{2}\Gamma(p)} , \tag{41}$$

where $E_R(p)$ is given by

$$E_R(p) = M - g^2 4\pi m \; P\int_0^\infty dx\sqrt{2mx}\frac{|\tilde{\Lambda}(x)|^2}{x_0 - x} . \tag{42}$$

The form of $\Gamma(p)$ in Eq. 41 is the same as in Eq. 39. Note the sign change again in the second term of Eq. 42 when compared with the form derived earlier in the model with positive metric Hilbert space.

The analytic properties of the scattering amplitude are unusual in the complex energy plane [15]. In addition to the cut along the positive real axis (also present in the model with positive metric Hilbert space) we find a complex conjugate pole pair on the *first* Riemann sheet. This is the manifestation of the complex ghost pair whose origin is traced to the state vector $|1;0\rangle$ with negative norm. When the interaction is switched on, the real eigenvalue M splits into a complex conjugate pair with two conjugate eigenvectors. For small g the phase shift $\delta(E)$ rapidly changes from π to 0 for energies $E \approx M$, near the ghost pole location. The negative time delay $t_D = d\delta(E)/dE \approx -\Gamma^{-1}$ is interpreted as time advancement in the emergence of the scattered wave. The time advancement of the scattered wave is a characteristic aspect of microscopic acausality effects in scattering amplitudes with complex singularities on the first Riemann sheet.

As I will explain in the nex part, microscopic acausality is not expected to lead to logically inconsistent macroscopic phenomena in relativistic higher derivative field theories, like producing a heavy Higgs particle at the SSC site before the accelerator is built (perhaps the U.S. Congress did not know this).

3.2 Relativistic Scattering Processes

In section 2 we derived the quantization rules for the higher derivative O(4) scalar field theory with quartic self-interaction. The Hilbert space of the model, which also describes the dynamics of the Higgs sector in the minimal Standard Model, is divided into two distinct parts. In the physical subspace the norm is positive and the energy eigenvalues of the stationary eigenvectors are real in *every* Lorentz frame. Physical wave packets in observable initial and final states of scattering processes are formed from the Hamiltonian eigenstates of the physical subspace. Ghost states with complex energy and non-positive norm are in the unobservable nonphysical part of the Hilbert space. Although complex conjugate ghost pairs can have positive norm and real total energy in some special Lorentz frame, their energy is complex in general Lorentz frames. Accordingly, conjugate ghost pairs are described by state vectors in the unobservable part of the Hilbert space.

We will study the scattering amplitudes in the Higgs phase of the model with spontaneous symmetry breaking. The spectrum is more complex than in the symmetric phase. There is a Higgs particle with mass m_H, and three massless Goldstone excitations with residual $O(3)$ symmetry. In addition, there

is a complex conjugate pair of heavy ghost states with the internal quantum numbers of the Higgs particle, and a three-component complex ghost pair which transforms as $O(3)$ triplet according to the quantum numbers of the Goldstone particles. The heavy masses of the Higgs ghost and the Goldstone ghost are split by the symmetry breaking mechanism.

The scattering amplitudes of physical states have unusual singularity structures. Consider the elastic scattering of two Goldstone particles ($W_L W_L$ scattering via the equivalence theorem [16]). The scattering amplitude has a cut in the invariant energy variable $s = (p_1 + p_2)^2$ along the real axis, starting at the origin. This cut is attributed to the contribution of intermediate Goldstone states to the imaginary part of the scattering amplitude. In addition, there are two complex poles at $s = \mathcal{M}^2$ and $s = \mathcal{M}^{*2}$ on the physical sheet (the Higgs particle appears as an ordinary resonance pole on the second sheet).

In the more complicated intermediate state of Fig. 1a the unphysical complex ghost state and a massles Goldstone particle generate branch point singularities at $s = \mathcal{M}^2$ and $s = \mathcal{M}^{*2}$ in the complex plane of the variable s. It can be shown

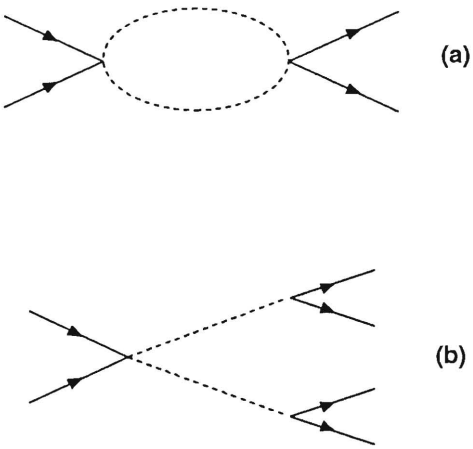

Figure 1: (a) The simplest Feynman loop diagram that probes unitarity in a nontrivial way is depicted. Internal dotted lines represent the full propagator which is a sum of Goldstone and ghost propagators with complex poles. The solid line designates massless Goldstone particles in the initial and final states. (b) Inelastic production of Goldstone particles through an intermediate ghost pair.

that the loop diagram is compatible with unitarity because the imaginary part of the corresponding scattering amplitude vanishes [15]. Although the ghost pair

does not appear in the physical final state, the ghost loop contributes to the real part of elastic scattering. The ghost loop also contributes to the renormalization group β-function in a non-trivial way. Cancellation effects between the ghost loop and ordinary particle loops will determine the evolution of the effective coupling constant of the scattering process at asymptotic energies.

The expected time advancement effects of the complex ghost pole on the outgoing wave packet can be estimated. The normalized incident wave packet χ^{in} is given by $|\chi^{in}|^2 \sim \frac{\Delta}{r^2} e^{-\Delta|r+t|}$ where r designates the distance between the colliding particles in the center of mass system and Δ is the momentum width of the incident wave packet. Assuming that $\Delta >> \gamma$ the ghost pole contribution to the outgoing wave packet χ^{out} has the intensity $|\chi^{out}|^2 \sim \frac{\gamma^2}{\Delta r^2} e^{-\gamma|r-t|}$ for $r - t >> \Delta^{-1}$. Since $t = 0$ is the time of collision, the intermediate ghost state acts in the scattering process as a peculiar resonance with time advancement in the emergence of the decay products. The scale of the time advancement is set by γ and remains undetectable with realistic wave packets which can be prepared in the initial states of realisitic experiments [5]. In the experimental mass distribution of the decay products the ghost will appear as a resonance state of approximate mass $Re\mathcal{M}$.

In the inelastic channel, schematically depicted in Fig. 1b, the mass distribution of the four Goldstone particles in the final state will show a pair of resonance bumps, although the ghost pair does not propagate in the intermediate state with macrosopic acausality effects. We estimated that the time advancement effects of the intermediate ghost pair in the outgoing scattered wave of elastic scattering, or in the decay products of the inelastic channel, are too small to observe.

In the next section I will apply the new theoretical developments to the investigation of the Higgs sector with a very heavy Higgs particle in the TeV mass range. Most of the simulation results are new and preliminary. I would like to thank my collaborators Karl Jansen and Chuan Liu for their permission to present the results [17].

4 Higgs Sector with Strong Interaction ?

In the minimal Standard Model with $SU(2)_L \times U(1)$ gauge symmetry the Higgs sector is described by a complex scalar doublet Φ with quartic self-interaction. The Higgs potential has the well-known form $V(\Phi^\dagger\Phi) = \frac{1}{2}m_0^2\Phi^\dagger\Phi + \lambda_0(\Phi^\dagger\Phi)^2$ where m_0^2 is a negative mass parameter and λ_0 designates the quartic coupling constant. The four real components of the complex scalar doublet Φ transform as a real vector Φ_α, $\alpha = 1, 2, 3, 4$, under O(4) symmetry transformations while

the Higgs potential remains invariant. In the limit where the gauge couplings and Yukawa couplings are neglected the quantization procedure for the higher derivative Higgs Lagrangian is the same what we discussed earlier.

Let me summarize again the main features of the spectrum. The O(4) model defined by the partition function of Eq. 32 has two phases. In the symmetric phase we find the original massive particle (with four components in the intrinsic O(4) space), and we also find a complex ghost pair with intrinsic O(4) symmetry whose mass scale is set by the Pauli-Villars mass parameter M. In the broken phase we find a Higgs particle with mass m_H, and three massless Goldstone excitations with residual O(3) symmetry. In addition, the 4-component heavy ghost particle and its complex conjugate partner also appear in the particle spectrum of the broken phase. One ghost state has the internal quantum numbers of the Higgs particle. The other three ghost states carry the internal quantum numbers of the Goldstone particles.

4.1 Lattice Action and Phase Diagram

We would like to investigate the existence of a very heavy Higgs particle and the feasibility of a strongly interacting Higgs sector. For non-perturbative computer simulations of the higher derivative Lagrangian we introduce a hypercubic lattice structure. The lattice spacing a defines a new short distance scale with the associated lattice momentum cut-off at $\Lambda = \pi/a$. We will have to work towards the large Λ/M limit in order to eliminate finite lattice effects from the already regulated and finite theory. After rescaling the continuum field components by $\Phi_\alpha = \sqrt{2\kappa}\phi_\alpha$ the euclidean lattice action has the form

$$S_E = \sum_x \left[-\kappa\, \phi_\alpha(\Box + M^{-4}\Box^3)\phi_\alpha + (1-8\kappa)\phi_\alpha\phi_\alpha + \lambda\, (\phi_\alpha\phi_\alpha - 1)^2 \right] \qquad (43)$$

where $\Box$ is the lattice Laplace operator, with the lattice spacing a set to one for convenience. The mass parameter and coupling constant are related to the hopping parameter κ and lattice coupling λ by $m_0^2 = (1 - 8\kappa - 2\lambda)/\kappa$, $\lambda_0 = \lambda/(4\kappa^2)$.

Stochastic algorithms exhibit severe critical slowing down for small values of the regulator mass M in the range $M < 1$. In this regime the $M^{-4}\Box^3$ term leads to a dramatic broadening of the frequency spectrum of the Fourier modes. We developed a Hybrid Monte Carlo algorithm with fast Fourier acceleration which solved the problem of critical slowing down very effectively.

The lattice model exhibits two phases, as expected. The symmetric phase with full $O(4)$ symmetry is separated by a second order phase transition line from the broken phase which has a residual $O(3)$ Goldstone symmetry for every

fixed value of λ in the (κ, M) plane. The phase diagram is shown in Fig. 2 in the $\lambda = \infty$ limit. Tuning the hopping parameter κ to the critical line for fixed M corresponds to the limit of trivial scalar field theory in the continuum. In this limit, the dimension eight operator $M^{-4}\phi_\alpha \Box^3 \phi_\alpha$ becomes irrelavant and while $m_H \to 0$ in lattice units, $M_R/m_H \to \infty$, so that ghost effects from the higher derivative term disappear. In our notation m_H is the physical Higgs resonance mass and M_R designates the real mass parameter of the exact ghost pole location in the complex plane. The continuum limit of the higher derivative theory without the underlying lattice structure is equivalent to the tuning of κ towards zero along a line of fixed M_R/m_H ratio. In this limit, which is depicted in Fig. 1 as the solid line, the higher derivative term $M^{-4}\phi_\alpha \Box^3 \phi_\alpha$ cannot be treated as an irrelevant operator in the Lagrangian.

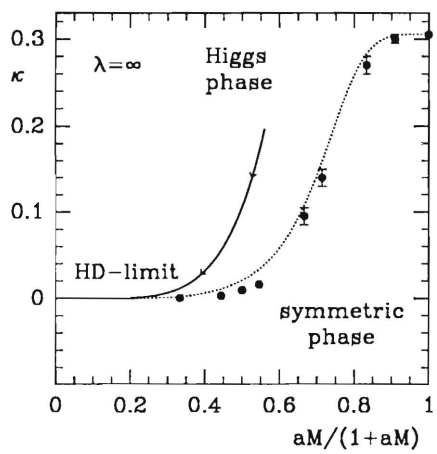

Figure 2: The phase diagram of the lattice model at infinite bare coupling. The dotted line is calculated in the large-N expansion. The solid line displays the fixed M_R/m_H ratio towards the continuum limit of the higher derivative theory.

4.2 Higgs Particle in the TeV Mass Range

Most of our computer simulations were performed on lattices which have cylinder geometry in the size range $16^3 \times 40$ to $20^3 \times 40$. On each lattice with a given parameter set 20,000 to 60,000 Hybrid Monte Carlo trajectories were accumulated in the Fourier transformed variables. On each time slice τ the radial Higgs field $\rho(\tau)$ and the $O(4)$ unit vector $n_\alpha(\tau)$ at zero three-momentum were

defined as

$$\overline{\phi_\alpha}(\tau) \equiv \frac{1}{L^3} \sum_{\mathbf{x}} \phi_a(\tau, \mathbf{x}) \equiv \rho(\tau) n_\alpha(\tau) \quad . \tag{44}$$

The renormalized vacuum expectation value v and the Higgs mass m_H were determined from the correlation functions $\langle n_\alpha(0) n_\alpha(\tau)\rangle$ and $\langle \rho(0)\rho(\tau)\rangle$.

The fitting procedure requires a theoretical understanding of the energy spectrum which is organized in the large volume limit according to inverse powers of the linear spatial size L. The tower of $O(4)$ rotator states forms the most densely spaced energy levels with level spacing of the order $(v^2 L^3)^{-1}$. The rotator states dominate the correlation function $\langle n_\alpha(0) n_\alpha(\tau)\rangle$ [18]. The Goldstone excitations have a level spacing which is of the order L^{-1}. In the correlation functions at zero three-momentum only Goldstone pairs can contribute which have rather large energies in the volumes we are considering. The largest level spacings correspond to radial Higgs excitations with a finite energy gap m_H above the ground state.

A simultaneous fit to m_H and v was performed on the data. The results are shown in Table 1 where all points correspond to a cylinder size of $16^3 \times 40$

Table 1: Simulation results at $M = 0.8$

κ	$\lambda_0/(10+\lambda_0)$	m_H	v	m_H/v
0.056	0.761	0.40(2)	0.058(2)	6.8(4)
0.056	0.761	0.32(2)	0.045(1)	7.1(6)
0.105	0.185	0.30(2)	0.066(2)	4.6(4)
0.115	0.086	0.21(3)	0.084(2)	2.5(4)

except for the second entry with size $20^3 \times 40$. The radial Higgs excitation in our simulations corresponds to a stationary state with real energy. Avoided level crossing with the lowest Goldstone pair of zero total momentum would only occur in larger spatial volumes. In our preliminary analysis the finite volume profile of the Higgs resonance was not developed. This rather crude approximation, where we identified the measured energy level of the radial excitation with m_H, is being subjected to systematic finite volume resonance analysis.

To compare our new results with earlier Higgs mass values, the ratio m_H/v is plotted as a function of the bare coupling constant in Fig. 3. If our preliminary results will not change after a more developed analysis, $m_H \geq 1$ TeV with a ghost location in the multi-TeV region implies the existence of a strongly interacting Higgs sector, a scenario which was excluded in previous lattice studies. Our heavy Higgs mass values in the TeV range do not represent conventional triviality bounds [19, 20, 21, 22, 23] at fixed bare coupling constants. Since

the ghost pair evades easy experimental detection without violating unitarity, Lorentz invariance, or any other sacred principles, a nonperturbative reinterpretation of the triviality Higgs mass bound becomes necessary.

To test the strongly interacting Higgs sector, we also determined the renormalized coupling constant in the symmetric phase. The preliminary results show stronger couplings in comparison with the lattice regulated $O(4)$ model.

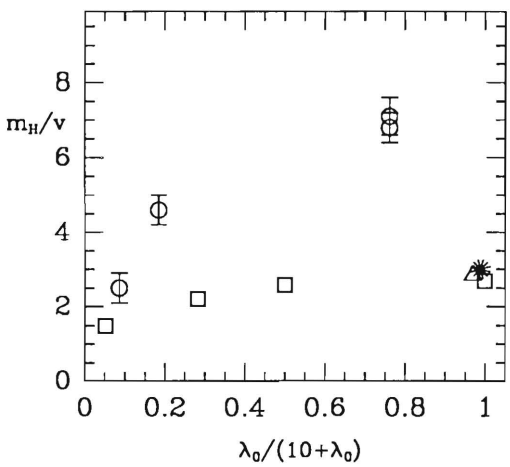

Figure 3: The circles are from our simulation results. They are compared with the simple $O(4)$ model on a hypercubic lattice [19, 20, 21] (squares), with Symanzik improved action on a hypercubic lattice [22] (star), and with dimension six interaction terms added on F_4 lattices [23] (triangle).

5 Quantum Gravity

It is well known that Einstein's theory of gravity fails the renormalizability test. An extended theory of general relativity with higher derivatives, based on a Lagrangian which is quadratic in the curvature, becomes a renormalizable field theory with very interesting mathematical and physical properties [6, 7].

5.1 Higher Derivative Lagrangian

The action of this extended gravitational theory has three independent terms,

$$S = -\int d^4x\sqrt{-g}\Big\{\frac{\gamma}{\kappa^2}R + \alpha R_{\mu\nu}R^{\mu\nu} - \beta R^2\Big\}\,, \tag{45}$$

where $\kappa^2 = 32\pi G$, and α, β, and γ are dimensionless numbers (coupling constants); $G = 6.67 \times 10^{-8} cm^3 g^{-1} s^{-1}$ is the fundamental Newtonian constant. In our notation $(- + ++)$ signature is used. The curvature tensor is defined by $R^{\lambda}_{\mu\alpha\nu} = \partial_\mu \Gamma^{\lambda}_{\mu\alpha} + ...$, and the Ricci tensor is given by $R_{\mu\nu} = R^{\lambda}_{\mu\lambda\nu}$. The Gauss-Bonnet topological invariance requires that the integral

$$\int d^4x \sqrt{-g} \Big(R_{\mu\nu\alpha\beta} R^{\mu\nu\alpha\beta} - 4 R_{\mu\nu} R^{\mu\nu} + R^2 \Big) \tag{46}$$

is a constant for a manifold with fixed topology. It actually vanishes for space-time manifolds which are topologically equivalent to flat space-time. Therefore, one can only construct two independent additions to the Einstein-Hilbert action which are quadratic in the curvature and fourth order in the derivatives. The addition of a cosmological term will be considered later.

The first term in Eq. 45 with $\gamma = 2$ corresponds to the original Einstein-Hilbert action with second order derivatives in the metric tensor $g_{\mu\nu}$. The last two terms, expressed in terms of fourth order derivatives of the metric tensor, are in the class of higher derivative field theories. Although the higher derivative terms in the action have very little effect on the low-frequency domain of classical experiments, at high frequencies they dominate the quantum behavior of the theory. They provide the stabilization of the divergence structure at short distances, with power-counting renormalizability of the quantum loops. In linearized perturbation theory the presence of the fourth order derivative terms leads to a graviton propagator with asymptotic momentum behavior q^{-4} reducing the degree of divergences to ≤ 4 in all graviton loops.

5.2 Gravitational Potential and Particle Content

It is straightforward to calculate the generalized gravitational field equations from the action of Eq. 45, augmented by a matter action [7]. For a point particle with $T_{\mu\nu} = \delta^0_\mu \delta^0_\nu M \delta^3(x)$, the gravitational field solution has the form

$$V = \frac{-\kappa^2 M}{8\pi\gamma r} + \frac{\kappa^2 M}{6\pi\gamma} \frac{e^{-m_2 r}}{r} - \frac{\kappa^2 M}{24\pi\gamma} \frac{e^{-m_0 r}}{r} \quad , \tag{47}$$

where $m_2 = \gamma^{1/2} (\alpha\kappa^2)^{-1/2}$ and $m_0 = \gamma^{1/2} [2(3\beta - \alpha)\kappa^2]^{-1/2}$. The Newtonian result at large r values is $V = -2GMr^{-1}$ which requires the choice $\gamma = 2$. As expected on dimensional grounds, the higher derivative terms only produce an appreciable effect at small distances from the source of the gravitational field, at a scale set by m_0 and m_2. At the origin, the Newtonian singularity $1/r$ is cancelled and V in Eq. 47 tends to a finite value $\kappa^2 M (24\pi\gamma)^{-1} (m_0 - 4m_2)$.

Eq. 47 has a Newtonian limit for positive values of m_0 and m_2. This constraint requires the positivity conditions

$$\alpha > 0, \qquad 3\beta - \alpha > 0 \tag{48}$$

on the couplings, eliminating the oscillatory behavior of $1/r$ terms at infinity. The domain in the coupling constant space which is consistent with the positivity conditions will be referenced later as the physical region of the couplings.

A detailed analysis of the linearized radiation in flat background space-time shows that there are eight dynamical degrees of freedom in the gravitational field. Two of these excitations correspond to the familiar massless spin-2 graviton. Five more correspond to a massive spin-2 particle with mass m_2. The eighth corresponds to a massive scalar particle with mass m_0. Although the linearized field energies of the massless spin-2 and massive scalar excitations are positive definite, the linearized energy of the massive spin-2 excitations is negative definite. This feature, as we have seen, is characteristic of higher-derivative models and requires quantization with indefinite metric in the Hilbert space. The same constraints on the couplings which kept the masses m_0 and m_2 positive also eliminates the possibility of tachyon excitations in the dynamical fields. These constraints will have a significant effect on the consistency of asymptotic freedom in the couplings at short distances.

5.3 Astronomical and Laboratory Tests

The static solution as given by Eq. 47 can be viewed as the gravitational potential of a star and it can be used to set limits on m_0 and m_2 from astronomical observations. It is perhaps surprising that the constraints are very weak even from high precision observations. For example, the orbital precession of Mercury is known to about 10^{-9} accuracy. The corrections from the higher derivative terms are proportional to $e^{-m_0 r}$ and $e^{-m_2 r}$ where the radius of Mercury's orbit, $\approx 5 \times 10^6$ km, has to be used for the value of r. This constraint on the masses is only $\approx 5 \times 10^{-11} cm^{-1}$.

It was pointed out [7] that there is no discontinuity in the coupling to light in the limit $m_0, m_2 \to \infty$. This implies that measurements of light bending by the sun do not yield more stringent constraints than other astronomical observations. One might expect that laboratory experiments on the Newtonian law of the gravitational $1/r^2$ force, as measured on the scale of meters, are more restrictive. Indeed, Cavendish type experiments are sensitive on the scale of a meter and they increase the lower bound on the two mass values to $m \geq 10^{-4} cm^{-1}$.

In our discussion I will assume that m_0 and m_2 are both in the mass range of the Planck scale $m_P = (\hbar c/G)^{1/2}$. The Planck mass $m_P = 1.3 \times 10^{19} GeV/c^2$ is more than thirty orders of magnitude larger than astrophysical, or laboratory lower bounds. There is no classical experiment which can signal the presence of higher derivative terms in this mass range. After a detailed understanding of the quantum theory, it will become a challenge to calculate more direct quantum effects of the new mass scale set by the higher derivative terms.

5.4 Renormalization and Unitarity

In the classical theory negative energy excitations were found in the linear approximation which signal wave propagation outside the light cone with acausal behavior. The quantization procedure preserves the positivity of the energy spectrum when indefinite metric is introduced in the Hilbert space of state vectors. A stable ground state is secured at the cost of states with negative norm.

The investigations of renormalization properties and the short distance behavior of quantum fluctuations are convenient in euclidean space, with a different parametrization of the gravitational action,

$$S = \int d^4x\sqrt{g}\Big\{ f^{-2}W - \frac{\omega}{3f^2}R^2 - \frac{2}{\kappa^2}R + 8\lambda/\kappa^4 \Big\} \ . \tag{49}$$

In this notation [24] sign $g_{\mu\nu} = +4$, $g = \det g_{\mu\nu}$, $W = R^2_{\mu\nu} - (1/3)R^2$, and $\lambda = \Lambda k^2$ is a dimensionless cosmological constant which was not introduced earlier. The parameters ω and f can be expressed in terms of α and β by simple relations.

The euclidean propagator in the quadratic approximation about flat euclidean background is given by

$$\Delta(q^2) = \frac{P_2}{q^2 + m_2^{-2}q^4} - \frac{P_0}{q^2 + m_0^{-2}q^4} \ , \tag{50}$$

where P_0 is the spin-zero projection operator and P_2 is the spin-two projection operator. The asymptotic behavior of the propagator is $\Delta(q^2) \approx 1/q^4$ and it can be shown that the loop expansion around the quadratic part of the euclidean action is renormalizable [7].

The particle content of the theory is exhibited by the propagator when written as a sum of simple pole terms,

$$\Delta(q^2) = \frac{P_2}{q^2} - \frac{P_2}{q^2 + m_2^2} - \frac{P_0}{q^2} + \frac{P_0}{q^2 + m_0^2} \ . \tag{51}$$

The first term in Eq. 51 is identified as the massless spin-two graviton. The second term is the massive spin-two particle which is quantized with negative norm

as evidenced by the negative sign of its contribution to the full propagator. The third term is not part of the spectrum, it is a gauge artifact of the quantization process. The last term describes the massive spin-zero particle with positive norm.

Since the massive spin-two particle can decay into a massless graviton pair, the Lee-Wick mechanism of higher derivative Quantum Electrodynamics was cited for the protection of the unitarity properties of the S-matrix in the presence of negative norm states [25]. The spin-two ghost state is split by the graviational interaction into a complex conjugate pole pair in graviton scattering amplitudes and the Lee-Wick mechanism is expected to maintain a logically consistent theory.

5.5 Asymptotic Freedom

The asymptotic behavior of quantum gravity with higher derivatives has been studied by several workers[26, 27, 24]. Only one of the three references came up with the correct answer, I believe.

In [27] the one-loop counterterms were calculated and the results of [26] were corrected. The analytic form of the one-loop counterterms allowed the calculation of the β-function to the same order. It was concluded that the theory is asymptotically free in the physically acceptable region of the coupling constants which is selected by the absence of tachyon instabilities in flat euclidean space. The condition for that requires a negative R^2 term in the euclidean action.

Although the conclusions of [27] that the tensor sector (the coupling constant of the W^2 term) exhibits asymptotic freedom is correct, the short distance behavior in the R^2 sector was changed completely [24]. In particular, the coupling constant associated with the R^2 term and the dimensionless cosmological constant have a triviality problem in the tachyon-free physical region of the couplings. Asymptotic freedom can be maintained only in the unphysical region of the couplings.

Although very little physics has been studied in the model, I am quite convinced that the picture of asymptotic freedom is basically correct. One has to choose the starting point of the loop expansion around the quadratic part of the euclidean action in de Sitter background. The expansion around flat euclidean space remains problematic and unstable. I hope to return to the continuation of the story at a future Johns Hopkins workshop.

Acknowledgements

I am greatful to the organizers of the workshop for the pleasant and informative meeting. This work was supported by the DOE under Grant DE-FG03-90ER40546 and by the Texas National Research Laboratory Commission under Grant RGFY03-206. The simulations of the higher derivative Higgs model were done at Livermore National Laboratory with DOE support for supercomputer resources.

References

[1] H. Weyl, Raum-Zeit-Materie (Springer-Verlag, Berlin) (1921) Chapter IV; A. Eddington, The Mathematical Theory of Relativity, 2nd ed. (Cambridge University Press, London) Chapter IV.

[2] F. Bopp, Ann. Phys. (Leipzig) 38 (1940) 345.

[3] B. Podolsky, Phys. Rev. 62 (1942) 68; B. Podolsky and P. Schwed, Rev. Mod. Phys. 20 (1948) 40.

[4] A. Pais and G. E. Uhlenbeck, Phys. Rev. 79 (1950) 145.

[5] T. D. Lee and G. C. Wick, Nucl. Phys. B9 (1968) 209; Phys. Rev. D2 (1970) 1033.

[6] R. Utiyama and B. DeWitt, J. Math. Phys. 3 (1962) 608.

[7] K. S. Stelle, Gen. Rel. Grav. 9 (1978) 353; Phys. Rev. D16 (1977) 953.

[8] M. Ostrogradski, Mem. Ac. St. Petersbourg, 4 (1850) 385.

[9] W. Pauli, Rev. Mod. Phys. 15 (175) 1943.

[10] K. Jansen, J. Kuti and C. Liu, Nucl. Phys. B (Proc. Suppl.) 30 (1993) 681.

[11] K. Jansen, J. Kuti and C. Liu, Phys. Lett. B309 (1993) 119; Phys. Lett. B309 (1993) 127.

[12] A. A. Slavnov, Nucl. Phys. B31 (1971) 301.

[13] S. W. Hawking, Quantum Field Theory and Quantum Statistics, edited by I. A. Batalin et al. (1987) 129.

[14] E. P. Wigner and W. F. Weisskopf, Z. Phys. 63 (1930) 62.

[15] C. Liu and J. Kuti, in preparation.

[16] B. W. Lee, C. Quigg and H. B. Thacker, Phys. Rev. D16 (1977) 1519.

[17] K. Jansen, J. Kuti, and C. Liu, preprint UCSD/PTH 93-39, and paper in preparation.

[18] A. Hasenfratz et al., Nucl. Phys. B356 (1991) 332.

[19] J. Kuti, L. Lin, Y. Shen, Nucl. Phys. (Proc. Suppl.) B 4 (1988) 397; Phys. Rev. Lett. 61 (1988) 678.

[20] M. Lüscher and P. Weisz, Phys. Lett. B212 (1988) 472.

[21] A. Hasenfratz et al., Nucl. Phys. B317 (1989) 81.

[22] M. Göckeler, H. Kastrup, T. Neuhaus and F. Zimmermann, Nucl. Phys. (Proc. Suppl.) B26 (1992) 516.

[23] U.M. Heller, H. Neuberger and P. Vranas, Nucl. Phys. B405 (1993) 557.

[24] I. G. Avramidy and A. O. Barvinsky, Phys. Lett. 159B (1985) 269.

[25] E. Tomboulis, Phys. Lett. 70B (1977) 361.

[26] J. Julve and M. Tonin, Nuovo Cimento 46B (1978) 137.

[27] E. S. Fradkin and A. A.Tseytlin, Phys. Lett. 104B (1981) 377; Nucl. Phys. B201 (1982) 469.

NAME	I D No.	M.S.

RETURN TO FERMILAB LIBRARY